Relativistic mean-field calculations of Λ and Σ hypernuclei

N. K. Glendenning
Nuclear Science Division, Lawrence Berkeley Laboratory, University of California, Berkeley, California 94720

D. Von-Eiff, M. Haft, H. Lenske, and M. K. Weigel
Sektion Physik der Ludwig-Maximilians-Universität München, Theresienstrasse 37/III, W-8000 München 2, Federal Republic of Germany

(Received 30 October 1992)

Single-particle spectra of Λ and Σ hypernuclei are calculated within a relativistic mean-field theory. The hyperon couplings used are compatible with the Λ binding in saturated nuclear matter, neutron-star masses, and experimental data on Λ levels in hypernuclei. The spin-orbit potentials for the hyperons and the influence of the ρ-meson field (isospin dependent interaction) are discussed.

PACS number(s): 21.80.+a

Hypernuclei are intrinsically interesting and are a potential source of information on the coupling constants of hyperons, which is of great relevance to other branches of physics. Of particular importance is the participation of strange particles in dense baryonic matter, since many questions in heavy-ion physics and astrophysics are related to this. The population of hyperons in dense matter will depend of course on their coupling constants relative to each other and to the nucleons. Strangeness production will also depend on the ratio of the system's time scale compared to that of the weak interaction, which is small for nuclear reactions, therefore conserving total strangeness, and long in astrophysical objects, therefore allowing the growth of net strangeness in neutron stars. The effect of hyperon populations on the electrical conductivity of neutron stars, hence on the decay rate of their magnetic field and their active lifetime as pulsars [1], and on the cooling rate of neutron stars [2,3] have been emphasized elsewhere.

As an important first step towards the understanding of these open problems we consider in this paper strangeness in the ground state of nuclei. Experimentally data on Λ hypernuclear levels have been so far the only source of information on hyperon couplings. Theoretical approaches to this spectroscopy range from nonrelativistic models [4] to the relativistic Hartree approximation (RHA) [5,6]. For the RHA one uses a Lagrangian with effective Λ couplings to the σ- and ω-meson fields. In Ref. [6] the Λ coupling constants (i.e., their relative strength to the corresponding nucleon couplings $x_\sigma = g_{\Lambda\sigma}/g_\sigma$ and $x_\omega = g_{\Lambda\omega}/g_\omega$) have been fitted to the experimental Λ hypernuclei spectra. However, treating x_σ and x_ω as independent parameters leads to a highly uncertain determination (correlation errors up to ±65% in Ref. [6]).

On the other hand, the contribution of the hyperons strongly influences the mass of neutron stars. In a recent publication [7] Glendenning and Moszkowski related the scalar and vector couplings of the Λ hyperon to its empirical binding in saturated nuclear matter [4] and thereby obtained compatibility of this binding energy with maximum neutron-star masses. In fact, the large correlation found in the least-squares fit mentioned above [6] reflects this relation of x_σ and x_ω to the Λ binding in nuclear matter. In summary, one finds that (1) neutron-star masses, (2) the Λ binding in saturated nuclear matter, and (3) Λ levels in hypernuclei are mutually compatible and rather narrowly constrain the Λ couplings.

Concerning Σ hypernuclei, up to now the experimental situation is not satisfactory. Σ hypernuclear production has been investigated at CERN, and later at Brookhaven and KEK, but the statistical accuracy of the available data is not very good because of the strong conversion that the Σ undergoes in the nucleus ($\Sigma N \rightarrow \Lambda N$). The controversial evidence for narrow Σ states ($\Gamma < 5-10$ MeV) is reviewed in Ref. [8]. In the absence of experimental evidence, theoretical investigations involving the Σ and higher mass hyperons have had to rely on some assumption concerning the couplings, of which universal hyperon coupling is plausible; i.e., all hyperons in the lowest octet have the same couplings as the Λ [7,9]. The prospects for significant advances in high resolution hypernuclear spectroscopy at CEBAF or at future facilities such as the proposed PILAC and KAON are discussed in Ref. [10].

It is the aim of this contribution to analyze Λ hypernuclei under consideration of the constraints (1)–(3) mentioned above and to extend such an investigation to Σ hypernuclei. Due to the paucity of experimental data, the results concerning Σ hypernuclei should be regarded as a first estimate.

For the nucleonic sector we use the well-known nuclear field theory Lagrangian including the nucleon couplings to the σ-, ω-, and ρ-meson fields [11] plus phenomenological σ self-interactions [12]. For the three charge states of the Σ hyperon we write the following Lagrangian [13,14]:

$$\mathcal{L} = \sum_{\Sigma} \bar{\psi}_\Sigma (i\gamma_\mu \partial^\mu - M_\Sigma + g_{\Sigma\sigma}\sigma - g_{\Sigma\omega}\gamma_\mu \omega^\mu)\psi_\Sigma - \bar{\Sigma}_{ij}\left[\frac{g_{\Sigma\rho}}{2}\gamma_\mu \Theta^\mu_{jk} + \frac{e}{2}\gamma_\mu A^\mu (\tau_3)_{jk}\right]\Sigma_{ki} , \quad (1)$$

where Σ_{ij} and Θ^{μ}_{ij} are the traceless 2×2 matrices

$$\Sigma_{ij}=\begin{pmatrix}\psi_{\Sigma^0} & \sqrt{2}\psi_{\Sigma^+}\\ \sqrt{2}\psi_{\Sigma^-} & -\psi_{\Sigma^0}\end{pmatrix} \tag{2}$$

and

$$\Theta^{\mu}_{ij}=\begin{pmatrix}\rho^{\mu}_0 & \sqrt{2}\rho^{\mu}_+\\ \sqrt{2}\rho^{\mu}_- & -\rho^{\mu}_0\end{pmatrix} . \tag{3}$$

The sum on Σ in the first line of Eq. (1) is over the charge states Σ^-, Σ^0, and Σ^+. The Euler-Lagrange equations then yield the Dirac equations for the Σ hyperons:

$$(i\gamma_\mu\partial^\mu-M^*_\Sigma-g_{\Sigma\omega}\gamma_\mu\omega^\mu-I_{3\Sigma}g_{\Sigma\rho}\gamma_\mu\rho^\mu_0 -I_{3\Sigma}e\gamma_\mu A^\mu)\psi_\Sigma=0 , \tag{4}$$

$$M^*_\Sigma=M_\Sigma-g_{\Sigma\sigma}\sigma , \tag{5}$$

where $I_{3\Sigma}$ denotes the third isospin component; i.e., $I_{3\Sigma}=-1,0,+1$ for Σ^-, and Σ^0, and Σ^+, respectively. This means that Eq. (4) already reflects the fact that within a RHA only the charge neutral component of the ρ-meson field, ρ^μ_0, yields a nonzero ground-state expectation value.

The Λ hyperon has isospin and charge zero and therefore cannot couple to the ρ-meson and electromagnetic fields. Hence, under the consideration of the universal hyperon coupling and the replacement of M_Σ by M_Λ in Eq. (5), the Λ Dirac equation equals the Σ^0 Dirac equation.

In the Lagrangian, Eq. (1), the hyperon-vector meson vertices are described by a coupling of magnetic type. As was pointed out in Refs. [15,16] and, more recently, also by Jennings [17] and Chiapparini *et al.* [18] this amounts to neglecting the anomalous magnetic moments of the hyperons. If they are taken into account, additional second-rank tensor contributions would appear [12–15]. The analysis of Brockmann [15], which resembles our approach, shows that the tensor contributions actually are of minor importance, influencing single-particle energies on a level of less than 1 MeV in most of the cases. In contrast, in Refs. [17,18] arguments were invoked for the dominance of the tensor coupling over the magnetic one. They are based on a SU(3)-symmetric direct coupling of the ω meson to the nonstrange quarks in the hyperon rather than to the hyperon as a whole.

Such processes contribute significantly only at small distances. Thus, large momentum transfers would be involved which are clearly beyond a mean-field theory. Also, the meson fields of an effective mean-field theory like the one used here implicitly include many-body effects and their relation to *free* meson fields is an interesting but yet undecided question. In this connection it is important to note that already the free physical ω meson has a strangeness content of about 10% due to the mixing with the Φ meson (see, e.g., Ref. [19]) and a magnetic coupling of a similar size to the strangeness in hyperons has to be expected.

In view of these open questions and since the present study is intended in the first place to explore the extension of the relativistic mean-field description to Σ hypernuclei, the tensor coupling for the vector mesons is neglected. An approach is used which was found to describe simultaneously Λ hypernuclei [5,6] and neutron stars [7] very well.

To calculate the hypernuclear spectra we made use of a technique similar to the so-called expectation-value method, which was successfully used within nonrelativistic and relativistic nuclear physics to incorporate shell effects into semiclassical densities and energies (see Refs. [20–22]): The Dirac-Hartree equations for the hyperons are solved only once with the meson fields of the corresponding nucleonic system, which are self-consistently determined within a relativistic Thomas-Fermi (RTF) approximation, as an input.

To check the validity of this approximation we recalculate the Λ single-particle spectra for the hypernuclei ${}^{40}_{\Lambda}$Ca and ${}^{208}_{\Lambda}$Pb with the parameters of Ref. [6] (parameter set I in Table I). The results for various Λ levels are displayed in Table II where our results are denoted by H^*. Compared with the fully self-consistent RHA results the H^* approximation systematically underestimates the Λ bindings which may be attributed to a surface energy that is somewhat too large within the RTF approach [23]. But as expected, the agreement is better for the larger mass number A and the deeper lying levels because in both cases the Thomas-Fermi assumption of locally constant fields is more valid. In conclusion, our results show a rather good agreement with those of Ref. [6], which gives confidence in the described scheme.

In the next step we calculate several Λ and Σ hypernuclei using a set of coupling constants from Ref. [7], which considers the constraints (1)–(3) mentioned above and in addition has been successfully used in the description of nuclear matter properties (parameter set II in Table I). The relative strength of the ρ-Σ coupling, $x_\rho=g_{\Sigma\rho}/g_\rho$, has been chosen to be equal to $x_\sigma=0.6$ which is central

TABLE I. Parameters of the two forces considered in the text. In both cases the nucleon mass $M=938$ MeV. For saturated nuclear matter the set II [7] yields energy per particle $E/A=-16.3$ MeV, density $\rho_0=0.153$ fm^{-3}, incompressibility $K=300$ MeV, effective mass $M^*/M=0.7$, and symmetry energy coefficient $a_{\rm sym}=32.5$ MeV. $C_i^2=g_i^2(M/m_i)^2$, $x_i=g_{Hi}/g_i$; $i=\sigma,\omega,\rho$; $H=\Lambda,\Sigma$.

	I [6]	II [7]
m_σ (MeV)	499.31	500
m_ω (MeV)	780	783
m_ρ (MeV)	763	770
M_Λ (MeV)	1116.08	1115
M_Σ (MeV)		1190
C^2_σ	348.26	266.40
C^2_ω	229.29	161.53
C^2_ρ	148.92	99.67
10^3b	2.2847	2.947
10^3c	−2.9151	−1.070
x_σ	0.464	0.600
x_ω	0.481	0.653
x_ρ		0.600

TABLE II. Comparison of our H^* results for various Λ levels in $^{40}_{\Lambda}$Ca and $^{208}_{\Lambda}$Pb with the fully self-consistent relativistic Hartree results from Ref. [6]. All quantities are in MeV.

	$^{40}_{\Lambda}$Ca		$^{208}_{\Lambda}$Pb	
Level	RHA [6]	H^*	RHA [6]	H^*
$1d_{3/2}$	−2.63	−1.17	−15.78	−15.03
$1d_{5/2}$	−3.76	−2.08	−16.12	−15.32
$1p_{1/2}$	−10.93	−8.75	−20.38	−19.42
$1p_{3/2}$	−11.61	−9.38	−20.51	−19.54
$1s_{1/2}$	−19.43	−16.90	−24.19	−23.23

to a rather narrow range required by the three constraints mentioned earlier concerning neutron star masses, hypernuclear levels, and the binding of the Λ in uniform matter [7]. The vector coupling corresponding to the above value of x_σ, which retains the correct Λ binding in nuclear matter, is $x_\omega = 0.568$ or 0.653 depending on the value of the effective nucleon mass at nuclear matter saturation, $m^*/m = 0.78$ or 0.7, respectively [7]. Alternately, one could have invoked vector dominance and chosen x_ρ to equal x_ω. From the numbers quoted, it is clear that the specific choice made can be said to accord with vector dominance within the uncertainty in the saturation value of the nucleon effective mass.

In Fig. 1 we show the contributions of the meson and electromagnetic fields to the hyperon self-energy for the nuclei ^{28}Si, ^{40}Ca, ^{90}Zr, and ^{208}Pb. The nonrelativistic reduction of the hyperon potential (for Λ and Σ^0 entirely, for $\Sigma^\pm$ mainly), given by the difference $g_{H\omega}\omega^0 - g_{H\sigma}\sigma$, $H = \Lambda, \Sigma$, is also displayed. It is worth noting that the small potential depths of ~30 MeV go along with a relatively smooth radial dependence (compared with nucleonic potentials), thereby additionally supporting the feasibility of the Thomas-Fermi meson fields. A similar behavior was found for $^{16}_{\Lambda}$O within the RHA calculations of Ref. [6]. In Figs. 2 and 3 we show the single-particle spectra of protons, neutrons, Λ, Σ^0, and Σ^+ hyperons for the nuclei ^{40}Ca and ^{208}Pb. Because of the smaller couplings the hyperon levels are considerably less bound than the corresponding nucleon levels. Looking at the Λ and Σ^0 single-particle energies, the larger M_Σ yields a smaller repulsive effect of the kinetic energy resulting in systematic stronger bindings for the Σ^0.

Dealing with hypernuclear states and their structure, one of the most interesting questions concerns the spin-orbit potential for the hyperons [10]. It is one of the great advantages of a relativistic treatment that the spin-orbit interaction is automatically included in the single-particle Dirac equation, and can be identified by means of a Foldy-Wouthuysen reduction. For example, looking at the charge neutral Λ and Σ^0 hyperons, both of which are

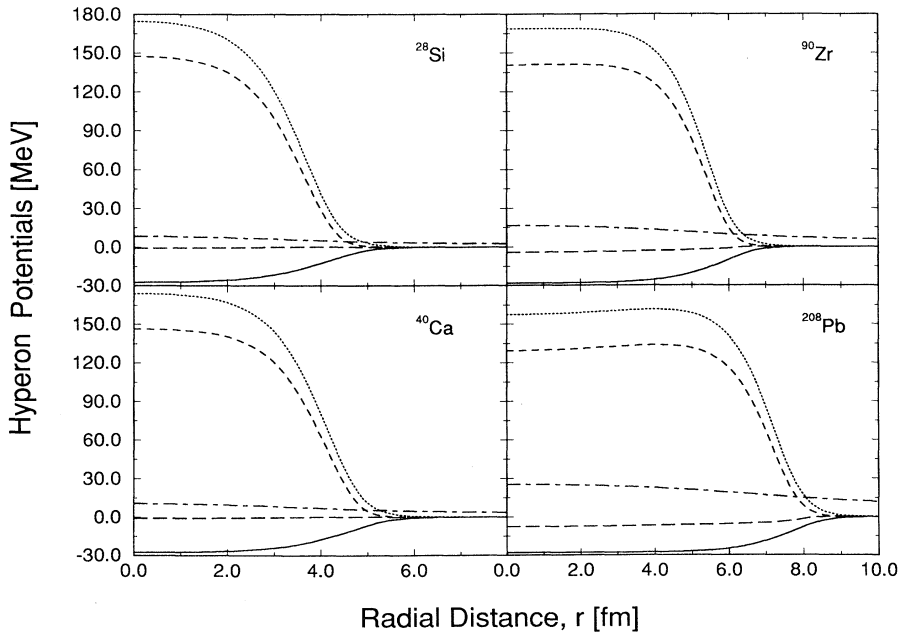

FIG. 1. Hyperon self-energy contributions $g_{H\sigma}\sigma$ (dotted lines), $g_{H\omega}\omega^0$ (dashed lines), $g_{\Sigma\rho}\rho_0^0$ (long-dashed lines), and eA^0 (dot-dashed lines) for the nuclei ^{28}Si, ^{40}Ca, ^{90}Zr, and ^{208}Pb. The nonrelativistic reduction of the hyperon potential is (for Λ and Σ^0 entirely, for $\Sigma^\pm$ mainly) given by the difference $g_{H\omega}\omega^0 - g_{H\sigma}\sigma$, which is represented by the solid lines, respectively. $H = \Lambda, \Sigma$ in the hyperon coupling constants.

TABLE III. Various Σ^-, Σ^0, and Σ^+ levels in ${}^{28}_{\Sigma}$Si, ${}^{40}_{\Sigma}$Ca, ${}^{90}_{\Sigma}$Zr, and ${}^{208}_{\Sigma}$Pb. All quantities are in MeV.

Level	${}^{28}_{\Sigma}$Si Σ^-	${}^{28}_{\Sigma}$Si Σ^0	${}^{28}_{\Sigma}$Si Σ^+	${}^{40}_{\Sigma}$Ca Σ^-	${}^{40}_{\Sigma}$Ca Σ^0	${}^{40}_{\Sigma}$Ca Σ^+
$1f_{5/2}$				−2.31		
$1f_{7/2}$				−3.43		
$2s_{1/2}$	−5.19	−0.43		−9.73	−2.57	
$1d_{3/2}$	−5.10			−10.29	−3.00	
$1d_{5/2}$	−6.19	−0.87		−11.31	−3.99	
$1p_{1/2}$	−13.97	−7.96	−2.07	−18.79	−10.82	−3.00
$1p_{3/2}$	−14.71	−8.69	−2.79	−19.37	−11.42	−3.60
$1s_{1/2}$	−23.22	−16.63	−10.11	−27.10	−18.54	−10.07
	${}^{90}_{\Sigma}$Zr			${}^{208}_{\Sigma}$Pb		
$1f_{5/2}$	−13.35	−4.03		−26.47	−12.40	
$1f_{7/2}$	−14.30	−5.00		−26.87	−12.87	
$2s_{1/2}$	−19.35	−9.28		−30.79	−15.76	−0.73
$1d_{3/2}$	−20.29	−10.52	−0.87	−31.57	−16.99	−2.70
$1d_{5/2}$	−20.88	−11.15	−1.53	−31.76	−17.24	−3.02
$1p_{1/2}$	−26.90	−16.61	−6.47	−36.25	−21.06	−6.22
$1p_{3/2}$	−27.16	−16.91	−6.80	−36.31	−21.15	−6.36
$1s_{1/2}$	−32.94	−22.05	−11.31	−40.44	−24.48	−8.94

not coupled to the ρ-meson field, the ratio of the spin-orbit splitting (Thomas terms) is

$$\frac{V^{\Sigma^0}_{\text{s.o.}}}{V^{\Lambda}_{\text{s.o.}}}=\frac{M^2_{\Lambda}}{M^2_{\Sigma}}=0.88\ . \tag{6}$$

This ratio is in good agreement with the corresponding values found in Refs. [16,24] within comparable models and is very well reproduced in the spectra of Figs. 2 and 3. Concerning the ratios of the spin-orbit splitting of the Σ^+ and Σ^0 hyperon to the proton and neutron, respectively, a simple expression similar to the one of Eq. (6)

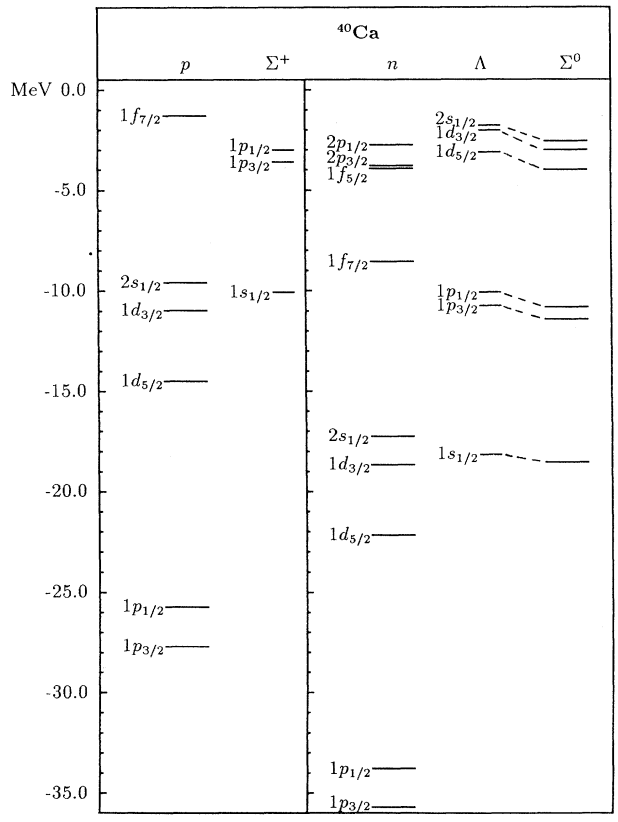

FIG. 2. The calculated proton, Σ^+, neutron, Λ, and Σ^0 single-particle spectrum for ^{40}Ca (parameter set II of Table I).

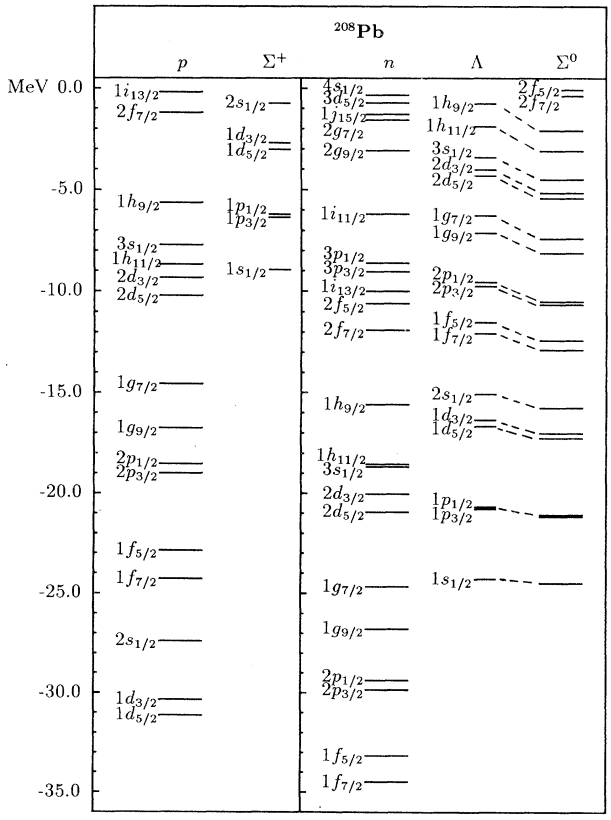

FIG. 3. Same as Fig. 2 for ^{208}Pb.

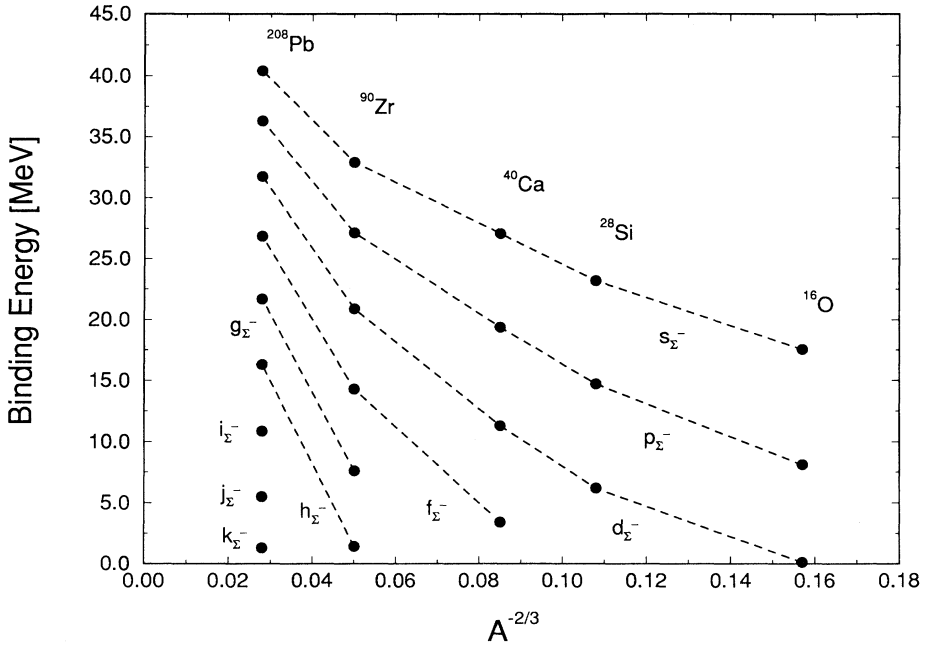

FIG. 4. Single-particle energies versus $A^{-2/3}$ for Σ^-. For each angular momentum the lowest lying state is plotted, respectively. The dashed lines are added to guide the eye.

cannot be given because of the different couplings. However, in the corresponding spectra of Figs. 2 and 3 we found a value of about ~ 0.34.

In Table III we compare various Σ^-, Σ^0, and Σ^+ levels for the $^{28}_{\Sigma}$Si, $^{40}_{\Sigma}$Ca, $^{90}_{\Sigma}$Zr, and $^{208}_{\Sigma}$Pb hypernuclei. Of course, the Coulomb force plays an important role: For symmetric ($N=Z$) hypernuclei, where the ρ-meson field is weak (it is nonzero because the proton and neutron density distributions differ due to the Coulomb interaction), we found the Coulomb shifts between Σ^- and Σ^0, or Σ^0 and Σ^+ states almost identical to the corresponding neutron-proton shifts in "normal" symmetric nuclei. The situa-

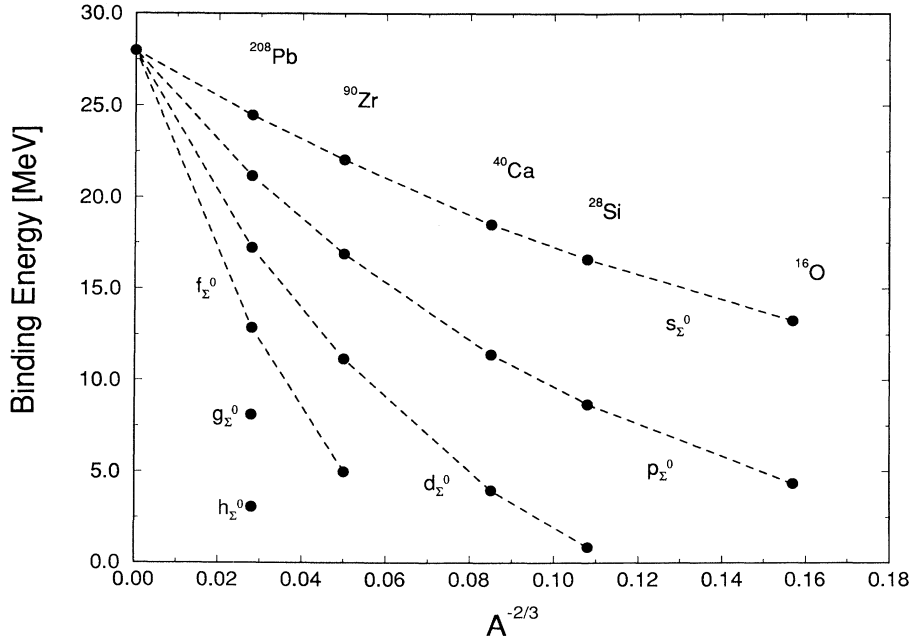

FIG. 5. Same as Fig. 4 for Σ^0. The value of -28 MeV for $A^{-2/3}=0.0$ represents the binding energy of the lowest Σ^0 level in saturated nuclear matter under the assumption of a universal hyperon coupling [4,7].

tion is somewhat different for hypernuclei with a neutron excess because then the effect of the ρ-meson field is not negligible anymore: For the Σ^- (Σ^+) the ρ-meson adds (subtracts) from the isoscalar part of the timelike repulsive vector field. The Σ^0 does not couple to the ρ field at all. To get an idea of the impact of the ρ-meson field we recalculated the asymmetric hypernuclei ${}^{90}_{\Sigma}$Zr and ${}^{208}_{\Sigma}$Pb with the ρ-Σ coupling switched off. For ${}^{90}_{\Sigma}$Zr we found the Σ^- (Σ^+) states stronger (weaker) bound by about 2.1–3.5 MeV; the corresponding range for ${}^{208}_{\Sigma}$Pb is 4.4–6.9 MeV. The fact that such relatively large ranges occur can be understood in terms of the rms radii: The lower bounds are for weakly bound states with large rms radii (e.g., the $1g_{9/2}$ Σ^- state with $r_{\rm rms}=5.40$ fm for ${}^{90}_{\Sigma}$Zr and the $3p_{1/2}$ Σ^- state with $r_{\rm rms}=6.97$ fm for ${}^{208}_{\Sigma}$Pb), while the upper bounds correspond to deep lying states with small rms radii (e.g., the $1s_{1/2}$ Σ^- states with $r_{\rm rms}=3.09$ fm for ${}^{90}_{\Sigma}$Zr and $r_{\rm rms}=3.68$ fm for ${}^{208}_{\Sigma}$Pb; the values for the rms radii are from the calculations with the ρ field switched on). As one can see, the influence of the ρ-meson field, whose range is determined by its mass m_ρ, weakens with increasing radial distances. (For neutrons and protons the situation is similar to the Σ^--Σ^+ pair but the effective ρ-nucleon coupling is weaker.)

Hence, the quantum hadrodynamical treatment of hypernuclei offers, by the possible inclusion of the ρ-meson field, a natural way to incorporate an isospin dependence into the Σ potential (i.e., a Lane potential), which was pointed out by Dover in Ref. [10] to be one of the most important questions of hypernuclear physics.

Finally, we show in Figs. 4–6 the single-particle energies of the Σ^-, Σ^0, and Σ^+ hyperons, respectively, versus $A^{-2/3}$, with A the mass number of the nuclei. For the Σ^- (Fig. 4) the attractive Coulomb potential allows the population of highly excited hypernuclear states (compared with the corresponding Σ^0 and Σ^+ hypernuclei as we will see later). Some of these states (the least bound) are such that the rms radii of the Σ^- wave functions are essentially outside the nucleus: Looking at ${}^{40}_{\Sigma^-}$Ca we found for the rms radii of the plotted s_{Σ^-}, p_{Σ^-}, d_{Σ^-}, and f_{Σ^-} states the values of $r_{\rm rms}=2.65$, 3.31, 3.89, and 4.76 fm, respectively, while the experimental charge rms radius for ^{40}Ca is $r_c\sim 3.48$ fm. Nevertheless, the d_{Σ^-} and f_{Σ^-} states are *hypernuclear* in nature as can be concluded from the corresponding level spacings in Table III. In Ref. [25] such states are called "*Coulomb-assisted hybrid bound* Σ^- *states.*"

For the charge neutral Σ^0 (Fig. 5) there is no Coulomb attraction and therefore the number of bound states decreases. The value of -28 MeV for $A^{-2/3}=0.0$ represents the binding energy of the lowest Σ^0 level in nuclear matter, which is under the assumption of a universal hyperon coupling the same as for the Λ particle [4,7]. As expected, the pattern of states shows the standard behavior as for Λ hypernuclei [6].

Turning finally to the discussion of the A dependence of the Σ^+ levels (Fig. 6) the situation is the following: Of course, now the Coulomb force is repulsive and the number of bound states further decreases compared with Σ^- and Σ^0 hypernuclei. The binding of the d_{Σ^+} state increases going from $A=90$ to $A=208$ as can be observed for the p_{Σ^+} state between $A=16$ and $A=28$. With increasing proton number Z the impact of the repulsive Coulomb potential grows leading to weaker bindings for the s_{Σ^+} and p_{Σ^+} states for $A=208$ compared with $A=90$. This latter effect is in accordance with the non-

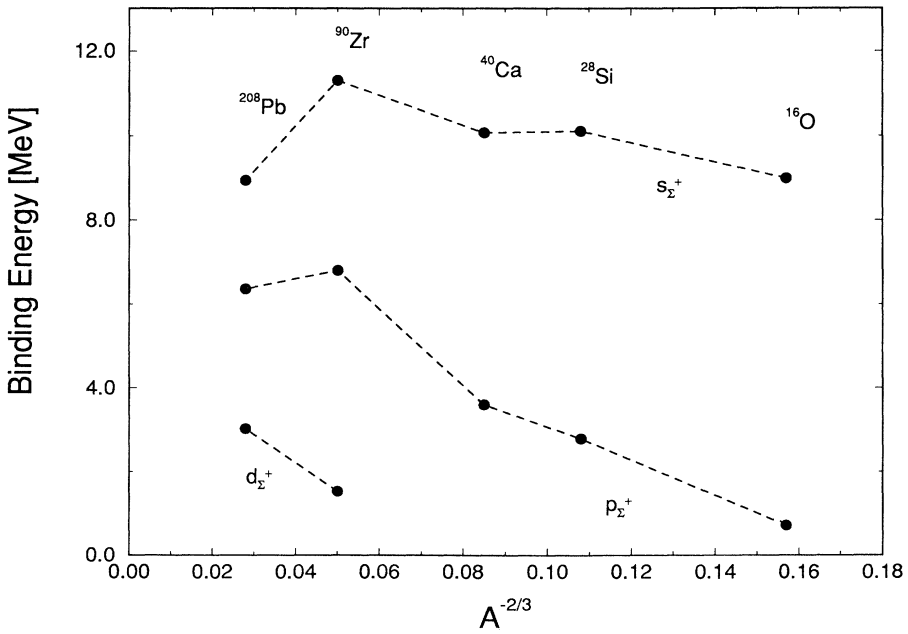

FIG. 6. Same as Fig. 4 for Σ^+.

relativistic calculations of Σ^+ hypernuclei by Divadeenam *et al.* (Ref. [26]; also presented in Ref. [8]), where a real potential well with a density dependence of the Skyrme form has been used. A similar behavior can be found within nonrelativistic Hartree-Fock Skyrme calculations for protons in "normal" nuclei, where the binding of the *d* levels strongly increases, whereas the *s* states nearly stay constant when going from $A=90$ to $A=208$ [27].

In the present calculations the broadening of the Σ hyperon states due to their decay to the Λ was neglected. In principle, the model can be extended to include the decay by introducing appropriate ΣΛ vertices. An important aspect of such an extended approach would be the possibility of investigating the decay of strange particles in the nuclear medium. In order to estimate the effects due to the conversion $\Sigma N \rightarrow \Lambda N$ the results of nonrelativistic potential models [28] may be taken as a guideline. In such approaches the decay is described schematically by an absorption potential for hyperons. The imaginary part of the self-energy effectively lowers the binding energy which can be understood in terms of the pole structure of the baryon propagator. Qualitatively a similar effect has to be expected also in a covariant description including the decay of the Σ hyperons. Thus the present results are likely to give *lower* bounds for the binding properties of the Σ particles in hypernuclei.

In conclusion, we performed relativistic mean-field calculations of Λ and Σ hypernuclei using an interaction that considers neutron-star masses, the Λ binding in saturated nuclear matter, and experimental Λ single-particle levels. Concerning the Σ couplings we assumed a universal hyperon coupling; i.e., all hyperons in the lowest octet couple to the meson fields as the Λ. We employed the so-called expectation-value method whose reliability was found to be sufficient compared with fully self-consistent RHA calculations. Analyzing the hypernuclear spectra, the spin-orbit potentials for hyperons and, in the case of Σ hypernuclei, the isospin dependence of the interaction were investigated. These two features are of particular interest in the current discussion concerning hyperon potentials in nuclei and are naturally incorporated into the relativistic quantum hadrodynamical model we used.

In the future it would be very valuable from the point of view of dense matter properties, and especially the structure of neutron stars, to have the assumption of a universal hyperon coupling confirmed by detailed precision experiments on Σ hypernuclei, and we hope that these calculations may possibly be of assistance as well as a stimulus to such experiments and the development of the necessary facilities.

ACKNOWLEDGMENTS

One of us (D.V.-E.) would like to thank the Ludwig-Maximilians-Universität München and the Deutsche Forschungsgemeinschaft for financial support. The authors wish to thank Professor W. Stocker for helpful discussions on the role of the surface energy. This work was supported by the Office of Energy Research, Office of High Energy and Nuclear Physics, Division of Nuclear Physics, of the U.S. Department of Energy under Contract No. DE-AC03-76SF00098.

[1] N. K. Glendenning, Astrophys. J. **293**, 470 (1985).
[2] O. V. Maxwell, Astrophys. J. **316**, 691 (1987).
[3] M. Prakash, M. Prakash, J. M. Latimer, and C. J. Pethick, Astrophys. J. **390**, L77 (1992).
[4] D. J. Millener, C. B. Dover, and A. Gal, Phys. Rev. C **38**, 2700 (1988).
[5] J. Boguta and S. Bohrmann, Phys. Lett. **102B**, 93 (1981).
[6] M. Rufa, J. Schaffner, J. Maruhn, H. Stöcker, W. Greiner, and P.-G. Reinhard, Phys. Rev. C **42**, 2469 (1990).
[7] N. K. Glendenning and S. A. Moszkowski, Phys. Rev. Lett. **67**, 2414 (1991).
[8] C. B. Dover, D. J. Millener, and A. Gal, Phys. Rep. **184**, 1 (1989).
[9] N. K. Glendenning, F. Weber, and S. A. Moszkowski, Phys. Rev. C **45**, 844 (1992).
[10] C. B. Dover, Nucl. Phys. **A547**, 27c (1992).
[11] M. H. Johnson and E. Teller, Phys. Rev. **98**, 783 (1955); H. P. Duerr, *ibid.* **103**, 469 (1956); B. D. Serot and J. D. Walecka, in *Advances in Nuclear Physics,* edited by J. W. Negele and E. Vogt (Plenum, New York, 1986), Vol. 16.
[12] J. Boguta and A. R. Bodmer, Nucl. Phys. **A292**, 413 (1977).
[13] J. D. Bjorken and S. D. Drell, *Relativistic Quantum Fields* (McGraw-Hill, New York, 1964).
[14] D. Lurié, *Particles and Fields* (Interscience, New York, 1968).
[15] R Brockmann, Phys. Lett. **104B**, 256 (1981).
[16] A. Bouyssy, Nucl. Phys. **A381**, 445 (1982).
[17] B. K. Jennings, Phys. Lett. B **246**, 325 (1990).
[18] M. Chiapparini, A. O. Gattone, and B. K. Jennings, Nucl. Phys. **A529**, 589 (1991).
[19] T. P. Cheng and L. F. Li, *Gauge Theory of Elementary Particle Physics* (Clarendon, Oxford, 1991), Chap. 4.
[20] O. Bohigas, X. Campi, H. Krivine, and J. Treiner, Phys. Lett. **64B**, 381 (1976).
[21] M. Brack, C. Guet, and H. B. Håkansson, Phys. Rep. **123**, 275 (1985).
[22] M. Centelles, X. Viñas, M. Barranco, S. Marcos, and R. J. Lombard, Nucl. Phys. **A537**, 486 (1992).
[23] D. Von-Eiff and M. K. Weigel, Phys. Rev. C **46**, 1797 (1992).
[24] M. Dillig, V. E. Herscovitz, and M. R. Teodoro, J. Phys. G **7**, L39 (1981).
[25] T. Yamazaki, R. S. Hayano, O. Morimatsu, and K. Yazaki, Phys. Lett. B **207**, 393 (1988).
[26] M. Divadeenam, T. E. Ward, and D. J. Millener, in *Intersections between Particle and Nuclear Physics,* Proceedings of a Conference held in Rockport, ME, 1988, edited by G. M. Bunce, AIP Conf. Proc. No. 176 (AIP, New York, 1988), p. 819.
[27] D. Vautherin and D. M. Brink, Phys. Rev. C **5**, 626 (1972).
[28] E. Oset, P. Fernández de Córdoba, L. L. Salcedo, and R. Brockmann, Phys. Rep. **188**, 79 (1990).